THE JOURNAL OF BIOLOGICAL CHEMISTRY VOL. 292, NO. 7, pp. 3005–3015, February 17, 2017

FOXO3 Transcription Factor Is Essential for Protecting Hematopoietic Stem and Progenitor Cells from Oxidative DNA Damage*

Received for publication, November 28, 2016, and in revised form, December 16, 2016 Published, JBC Papers in Press, December 19, 2016, DOI 10.1074/jbc.M116.769455

Carolina L. Bigarella[‡1], Jianfeng Li[§], Pauline Rimmelé[‡], Raymond Liang[‡¶2], Robert W. Sobol[§3], and Saghi Ghaffari[‡¶‖‡‡4]**

*From the [‡]Department of Cell, Developmental and Regenerative Biology, Icahn School of Medicine at Mount Sinai, New York, New York 10029, the [§]Department of Oncologic Sciences, University of South Alabama Mitchell Cancer Institute, Mobile, Alabama 36604, the [¶]Developmental and Stem Cell Biology Multidisciplinary Training Area, [‖]Department of Medicine, Division of Hematology and, Oncology, **Black Family Stem Cell Institute, and [‡‡]Tisch Cancer Institute, Icahn School of Medicine at Mount Sinai, New York, New York 10029*

Edited by Xiao-Fan Wang

Accumulation of damaged DNA in hematopoietic stem cells (HSC) is associated with chromosomal abnormalities, genomic instability, and HSC aging and might promote hematological malignancies with age. Despite this, the regulatory pathways implicated in the HSC DNA damage response have not been fully elucidated. One of the sources of DNA damage is reactive oxygen species (ROS) generated by both exogenous and endogenous insults. Balancing ROS levels in HSC requires FOXO3, which is an essential transcription factor for HSC maintenance implicated in HSC aging. Elevated ROS levels result in defective *Foxo3*$^{-/-}$ HSC cycling, among many other deficiencies. Here, we show that loss of FOXO3 leads to the accumulation of DNA damage in primitive hematopoietic stem and progenitor cells (HSPC), associated specifically with reduced expression of genes implicated in the repair of oxidative DNA damage. We provide further evidence that *Foxo3*$^{-/-}$ HSPC are defective in DNA damage repair. Specifically, we show that the base excision repair pathway, the main pathway utilized for the repair of oxidative DNA damage, is compromised in *Foxo3*$^{-/-}$ primitive hematopoietic cells. Treating mice *in vivo* with *N*-acetylcysteine reduces ROS levels, rescues HSC cycling defects, and partially mitigates HSPC DNA damage. These results indicate that DNA damage accrued as a result of elevated ROS in *Foxo3*$^{-/-}$ mutant HSPC is at least partially reversible. Collectively, our findings suggest that FOXO3 serves as a protector of HSC genomic stability and health.

The accumulation of damaged DNA compromises the genomic stability of hematopoietic stem cells (HSC)[5] (1) and may promote hematological malignancies, specifically with age (2, 3). Reactive oxygen species (ROS) are one of the major insults that induce DNA damage (4), including in normal hematopoietic and leukemic stem cells. ROS are generated both endogenously by cell metabolism or expression of oncoproteins and exogenously by ionizing radiation and genotoxic drugs (1, 5, 6). ROS induce single and double strand DNA breaks as well as various species of oxidized nucleotides and are implicated in the pathophysiology of hematological malignancies (7). Thus, modulations of ROS may be used therapeutically (7, 8). Cells, with distinct kinetics, constantly repair oxidative damage using mainly the base excision repair (BER) pathway (9). The relatively low levels of endogenous ROS in HSC restrict damage to DNA (10); however, the impact of increasing ROS levels on HSC DNA remains relatively unexplored (11). Importantly, the mechanism of oxidative DNA damage repair in primitive hematopoietic cells remains poorly understood.

The transcription factor FOXO3 of the Forkhead family with four (FOXO1, FOXO3, FOXO4, and FOXO6) related members maintains HSC quiescence by ensuring low levels of ROS (12, 13). FOXOs belong to an evolutionarily conserved family of transcription factors that exert critical functions in the regulation of aging and longevity, including humans (14, 15). FOXOs are phosphorylated and inhibited mainly by AKT kinase downstream of the PI3K-signaling pathway. In addition to phosphorylation by AKT and other kinases, FOXOs are modified by a variety of post-translational modifications that together determine FOXOs' functional output (14). Notably, in hematopoietic stem and progenitor cells and in embryonic stem cells, AKT is not the dominant regulator of FOXO function (16–20). FOXOs are involved in an array of fundamental biological pro-

* This work was supported in part by National Institutes of Health Grants CA148629 and ES025138 (to R. W. S.) and CA205975 and HL116365, Myeloproliferative Neoplasm Foundation, Tisch Cancer Institute, and American Society of Hematology (to S. G.). R. W. S. is a scientific consultant for Trevigen, Inc. The content is solely the responsibility of the authors and does not necessarily represent the official views of the National Institutes of Health.
[1] Supported in part by a Roche Translational and Clinical Research Center-Young Investigator award.
[2] Supported by National Institutes of Health Grant T32 GM08553-13 and an American Heart Association fellowship.
[3] An Abraham A. Mitchell Distinguished Investigator.
[4] To whom correspondence should be addressed: Dept. of Cell, Developmental and Regenerative Biology, Icahn School of Medicine at Mount Sinai, New York, NY 10029. Tel.: 212-659-8271; Fax: 212-80-6740; E-mail: saghi.ghaffari@mssm.edu.

[5] The abbreviations used are: HSC, hematopoietic stem cell; ROS, reactive oxygen species; HSPC, hematopoietic stem and progenitor cell; NAC, *N*-acetylcysteine; BER, base excision repair; NER, nucleotide excision repair; BM, bone marrow; 8-OHdG, 8-hydroxyguanosine; TBI, total body irradiation; Gy, gray; MEF, mouse embryonic fibroblast; pol, polymerase; QRT, quantitative RT; 7-AAD, 7-aminoactinomycin D; PE, phycoerythrin; IR, ionizing radiation; HR, homologous recombination.

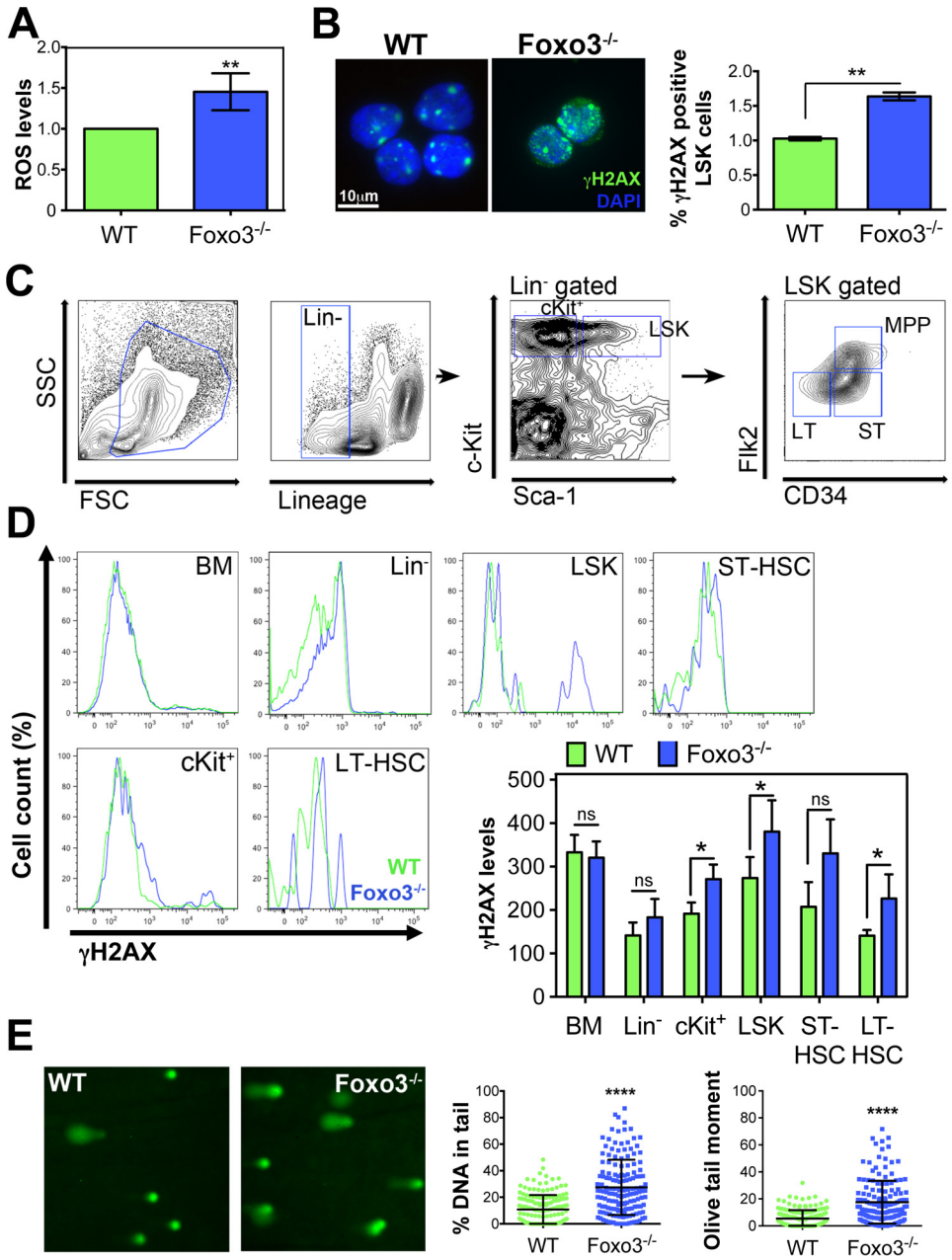

FIGURE 1. ***Foxo3*$^{-/-}$ hematopoietic stem and progenitor cells accumulate DNA damage at the steady state.** *A*, ROS levels in WT *versus Foxo3*$^{-/-}$ LSK cells (fold change of FITC fluorescence geometric mean normalized to that of WT). *B*, representative images of WT and *Foxo3*$^{-/-}$ FACS-sorted LSK cells stained with an anti-γH2AX antibody (*left panels*) and quantification of the percentage of positive cells (foci number >6) ($n \geq 40$ cells analyzed per condition, two independent experiments). **, $p < 0.001$. *C*, representative FACS plots for the gating strategy to analyze hematopoietic stem (LT and ST-HSC enriched in Lin$^-$Sca1$^+$cKit$^+$ (LSK) population) and progenitor (Lin$^-$cKit$^+$) cells. *SSC*, side scatter; *FSC*, forward scatter. *D*, flow cytometry analysis of γH2AX positivity in gated nucleated BM cells, lineage negative (*Lin*−), LSK, and c-Kit$^+$ myeloid progenitors, as well as in LT-HSC (Lin$^-$Sca1$^+$c-Kit$^+$Flk2$^-$CD34$^-$) and ST-HSC (Lin-Sca1$^+$c-Kit$^+$Flk2$^-$CD34$^+$) ($n \geq 4$ mice per group). *E*, comet assay of freshly isolated WT and *Foxo3*$^{-/-}$ LSK cells. % DNA in tail and Olive tail moment parameters were used to quantify the DNA breaks levels. Data expressed as mean ± S.D. (*A, B, D,* and *E*) Student's *t* test. *, $p < 0.05$; **, $p < 0.001$; ***, $p < 0.0002$; ****, $p < 0.0001$; *ns*, not significant.

cesses, including the regulation of metabolism and oxidative stress, cell cycle, apoptosis, and DNA repair (14, 15).

Loss of FOXO3 results in oxidative stress-mediated myeloproliferation that does not progress, at least not rapidly enough to have been detected, toward leukemia (12, 13, 21). FOXO3 is intimately involved in hematopoietic malignancies, as FOXO3 is found in chromosomal translocations of human acute myeloid leukemia (22) and is inhibited in malignant hematopoietic cells (18, 23–28). Despite these observations, FOXO3 is also required for the maintenance of both mouse and human leukemic stem cells (29–31). In addition, FOXO3 is implicated in HSC aging (32–34) and in stem cell pluripotency (16). Given the importance of DNA damage response for aging and malignancies of stem cells, we sought to explore the potential FOXO3 function in the regulation of DNA damage response in HSC.

Here, we show that FOXO3, which is essential for the regulation of oxidative stress in HSC (12, 13, 21, 35), is a key factor

in the primitive hematopoietic cell DNA damage response, specifically in base excision repair, and it protects HSPC from oxidative DNA damage under homeostasis. These findings raise the possibility that DNA damage accrual as a result of loss of FOXO3 function, as may occur with age, promotes HSC aging (32–34), predisposes HSPCs to premature aging, and/or contributes to hematopoietic stem cell malignant transformation (18, 23, 29, 30).

Results

Foxo3$^{-/-}$ Hematopoietic Stem and Progenitor Cells Accumulate Oxidative DNA Damage at the Steady State—Foxo3$^{-/-}$ LSK cells (Lin$^-$Sca1$^+$c-Kit$^+$) enriched for HSC accumulate ROS under homeostasis (Fig. 1*A*) (12, 13) as a result of defective anti-oxidant enzyme expression and mitochondrial function (12, 13, 36). Elevated ROS are associated with loss of *Foxo3$^{-/-}$* HSC quiescence (12, 13) and a delay at the G_2/M cell cycle checkpoint (13). We evaluated whether elevated ROS result in defective DNA integrity that contributes to cell cycle abnormalities of *Foxo3$^{-/-}$* HSC.

Under homeostatic conditions, a significantly higher fraction of freshly isolated *Foxo3$^{-/-}$* LSK cells exhibited enhanced phosphorylation of histone H2AX variant (γH2AX) (Fig. 1*B*), a sensor of DNA double strand breaks (37). A highly elevated level of damaged DNA was detected in *Foxo3$^{-/-}$* HSPC by both γH2AX immunofluorescence staining, in which cells with more than six nuclear foci were considered as positive, and the more sensitive flow cytometry assay, which enabled the quantification of the amount of damage (Fig. 1*B*, $n > 40$ cells analyzed per condition and Fig. 1*C*; $n = 5$, * $p < 0.05$). Damaged DNA accumulated in *Foxo3$^{-/-}$* HSPC subpopulations, including long term repopulating HSC (LT-HSC; LSK Flk2$^-$CD34$^-$) and c-Kit$^+$ (Lin$^-$Sca1$^-$c-Kit$^+$) multipotent progenitor cells but not in *Foxo3$^{-/-}$* total bone marrow (BM) control cells (Fig. 1,*C* for gating strategy, and *D*; $n = 4$ per genotype); although γH2AX was relatively increased in lineage negative cells depleted of mature blood cells and enriched for hematopoietic stem and progenitor cells, it did not reach significance in the samples evaluated. Using alkaline single-cell gel electrophoresis (comet assay), we further visualized the damage to single strand DNA and quantified an approximate 3-fold increased damage level in FACS-sorted *Foxo3$^{-/-}$ versus* wild type (WT) LSK cells by the use of (38) % of DNA in Tail and Olive tail moment parameters (Fig. 1*E*; $n = 6$). These results confirmed the increased amount of damaged DNA in *Foxo3$^{-/-}$* HSPC.

To evaluate whether ROS were involved in the accumulation of DNA damage in *Foxo3$^{-/-}$* HSPC, we used the FLARE hOGG1 comet assay that specifically detects oxidative DNA damage. This approach showed that oxidative DNA damage is significantly increased in freshly isolated *Foxo3$^{-/-}$ versus* WT HSPC (Fig. 2*A* and *B*, representative comet images and quantification). Using a specific probe that detects the main DNA oxidation lesion, 8-hydroxyguanosine (8-OHdG), by flow cytometry, we noted 8-OHdG levels were increased in *Foxo3$^{-/-}$* LSK cells as compared with WT cells (Fig. 2*C*), although the difference did not reach significance in the replicates analyzed ($n = 3$). Altogether, these results indicate that *Foxo3$^{-/-}$* HSPC DNA accumulates high levels of oxidative insults.

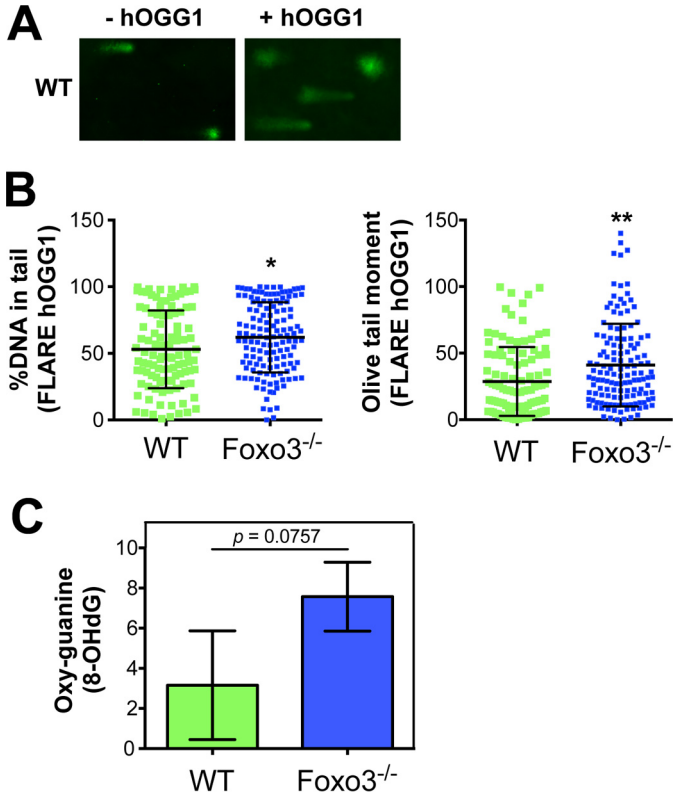

FIGURE 2. **DNA damage accumulation in *Foxo3$^{-/-}$* HSPC is from oxidative origin.** *A,* representative images of WT cells submitted to comet assay without hOGG1 (−*hOGG1*) or treated with hOGG1 (FLARE comet assay). *B,* FLARE-hOGG1 comet assay in freshly isolated LSK cells. *C,* 8-OHdG levels were analyzed by FACS in WT and *Foxo3$^{-/-}$* LSK cells ($n = 3$; geometric mean of fluorescence values ($\times 10^3$) are shown). Data are expressed as mean ± S.D. Student's *t* test. *, $p < 0.05$; **, $p < 0.001$.

Scavenging ROS by NAC Decreases Foxo3$^{-/-}$ HSPC DNA Damage and Corrects the G_2/M Delay—To investigate whether ROS have any functional role in the accumulation of DNA damage, mice were treated *in vivo* with NAC (100 mg/kg/day), a source of glutathione for 14 days (Fig. 3*A*, *schematic*). As anticipated, NAC treatment normalized ROS levels in *Foxo3$^{-/-}$* LSK cells without any significant impact on WT cells (Fig. 3*B*) (13). Notably, NAC treatment led to a 2-fold decrease of γH2AX levels in *Foxo3$^{-/-}$*-treated as compared with non-treated LSK cells ($n = 3$ per group; $p < 0.05$) (Fig. 3*C*). In addition, the levels of DNA breaks in *Foxo3$^{-/-}$* LSK cells, as quantified by the % Tail DNA and the Olive tail moment, were significantly reduced (2-fold) in response to NAC (Fig. 3*D*, quantification in the *right panel*). Despite normalized ROS levels (Fig. 3*B*), the % Tail DNA ($p < 0.0007$) and the Olive tail moment ($p < 0.00001$) remained significantly higher in NAC-treated *Foxo3$^{-/-}$* LSK cells as compared with WT controls (Fig. 3*D*), raising the possibility that not all damage to *Foxo3$^{-/-}$* LSK DNA resulted from elevated ROS.

In addition to reducing DNA damage, NAC treatment normalized the defective *Foxo3$^{-/-}$* cell cycle parameters (Fig. 4). Increased numbers of LSK cells isolated from NAC-treated *Foxo3$^{-/-}$* mice were in the G_0 and G_1 phases of the cell cycle and released from the G_2/M delay. The decreased frequencies of *Foxo3$^{-/-}$* LSK cells that incorporated BrdU *in vivo* (Fig. 4, *A* and *B*) and of *Foxo3$^{-/-}$* LT-HSC (LSK-CD34$^-$) Ki67-positive

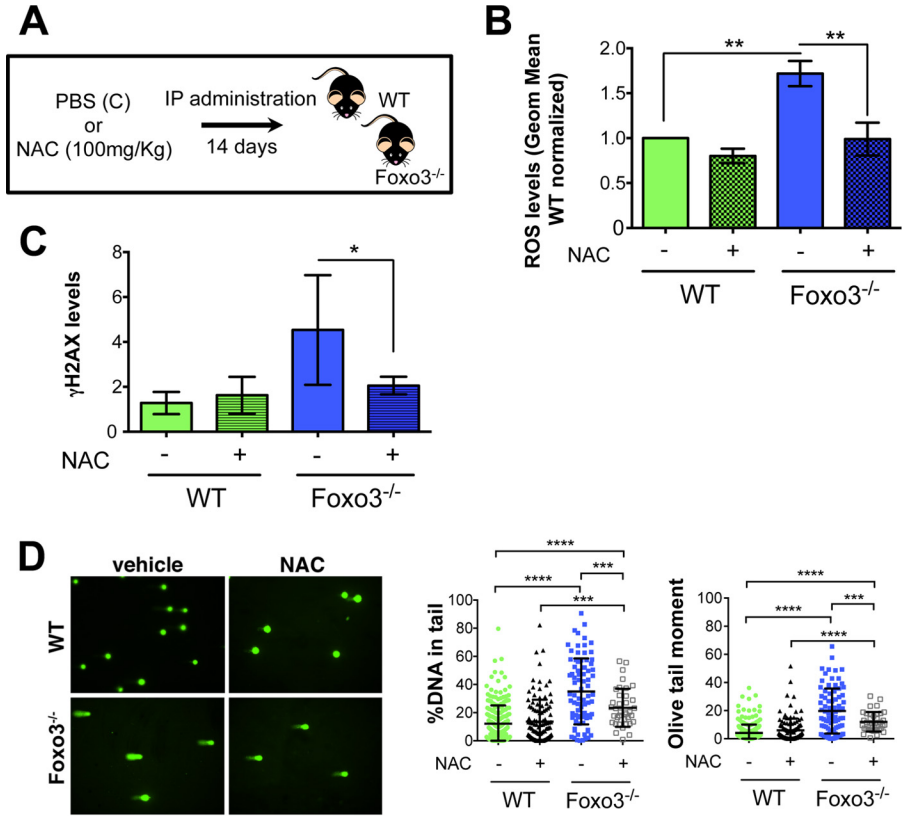

FIGURE 3. **NAC treatment reduces DNA damage accumulation in *Foxo3*$^{-/-}$ HSPC.** *A,* schematic representation of the NAC treatment to which WT and *Foxo3*$^{-/-}$ mice were submitted for 14 days. *IP,* intraperitoneal. *B,* analysis of dichlorofluorescein staining of WT and *Foxo3*$^{-/-}$ LSK cells isolated from mice that were treated with NAC for 14-days (geometric mean values normalized to that of WT). *C,* γH2AX levels were analyzed by FACS after NAC treatment ($n = 6$ per group, two independent experiments). *D,* alkaline comet assay analysis of FACS-sorted LSK cells from control and NAC-treated animals ($n \geq 100$ cells analyzed per group, two independent experiments). Representative images (*left panels*) and DNA break levels quantification by %DNA in Tail and Olive tail moment (*right panels*). Data are expressed as mean ± S.D. Student's *t* test. *, $p < 0.05$; **, $p < 0.001$; ***, $p < 0.0002$; ****, $p < 0.0001$.

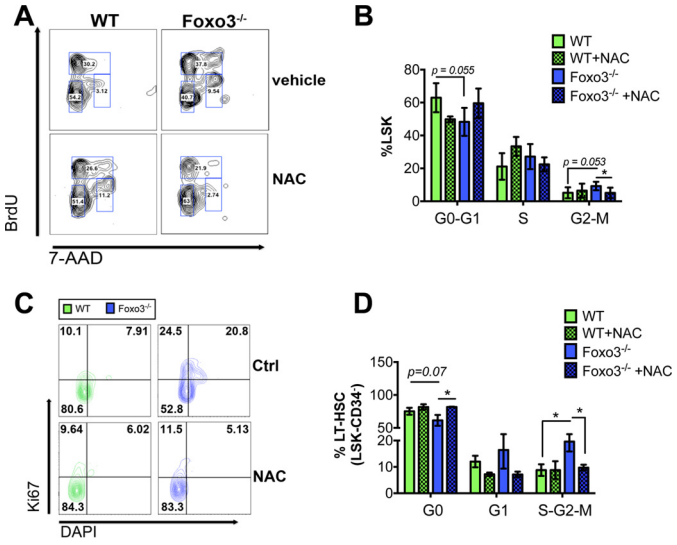

FIGURE 4. **NAC treatment corrects the defective cell cycle of *Foxo3*$^{-/-}$ HSPC.** Cell cycle analysis on freshly isolated BM cells from WT and *Foxo3*$^{-/-}$ mice treated for 14 days with NAC. *A,* representative FACS plots of BrdU staining, and *B* quantification of the percentage of LSK cells from control (vehicle) and NAC-treated mice in G_0-G_1, S, or G_2-M cell cycle phases. *C,* representative FACS plots of Ki67-DAPI staining on gated LSK-CD34$^-$ cells; *D,* quantification of the percentage of cells in G_0, G_1, or S-G_2-M cell cycle phases. $n = 6$ per group, two independent experiments. Data expressed as mean ± S.D. Student's *t* test .*, $p < 0.05$.

were comparable (Fig. 4, *C* and D). These combined results suggest that the block of cell cycle progression, G_2/M delay, in *Foxo3*$^{-/-}$ HSPC is due to ROS-mediated DNA damage.

Defective DNA Repair Machinery in Foxo3$^{-/-}$ *HSPC Contributes to DNA Damage Accumulation*—A number of key genes of BER, including DNA polymerase β (*polB*), X-ray repair cross-complementing protein 1 (*Xrcc1*), and DNA Ligase 1 (*Lig1*), were significantly down-regulated in *Foxo3*$^{-/-}$ LSK cells (Fig. 5*A*). Other genes implicated in nucleotide excision repair (NER), were also significantly reduced in *Foxo3*$^{-/-}$ LSK cells (Fig. 5*A*). Altogether, these results raise the possibility that the key pathways implicated in oxidative DNA damage repair may also be compromised in *Foxo3*$^{-/-}$ HSPC.

To address whether DNA in LSK cells that lack FOXO3 were preferentially susceptible to ROS elevation, we exposed these cells to 100 μM hydrogen peroxide for 1 h (Fig. 5*B*, *schematic*). This treatment led to significantly higher DNA breaks in *Foxo3*-deficient LSK cells as compared with their WT counterparts. The results were relatively similar when analyzed by either the standard or the FLARE hOGG1 comet assays (Figs. 5, *C* and *D*); the FLARE assay detected a more exacerbated DNA damage (Fig. 5*D*), suggesting increased sensitivity to removal of base damage such as those removed by the OGG1 DNA glycosylase. These findings indicate that the repair of oxidative DNA insults

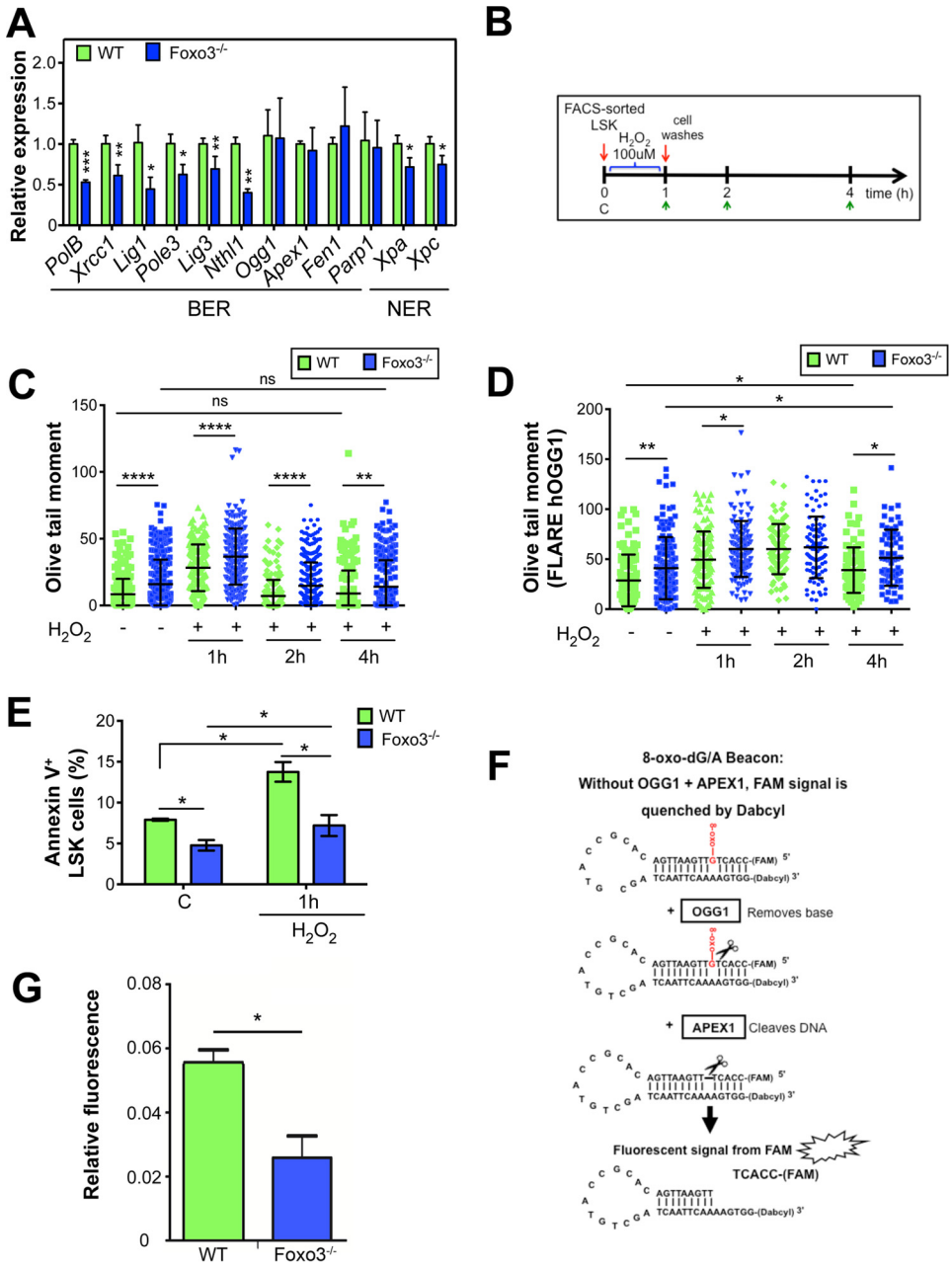

FIGURE 5. **Defective DNA repair machinery in *Foxo3*$^{-/-}$ HSPC contributes to DNA damage accumulation**. *A,* QRT-PCR analysis of expression of oxidative DNA repair (BER and NER) genes in freshly isolated HSPC. *Actnb* was used as internal control, and expression was normalized to the WT samples. *B,* schematic of FACS-sorted WT and *Foxo3*$^{-/-}$ LSK cells treated *ex vivo* with 100 μM H_2O_2. Cells were analyzed by alkaline comet assay (*C*) and comet FLARE-OGG1 (*D*) at the indicated time points shown by *green arrows* (1, 2, or 4 h after treatment). *E,* flow cytometry analysis of apoptosis using annexin V-binding in freshly isolated LSK cells treated for 1 h with 100 μM H_2O_2. *F,* schematic representation of the OGG1 activity assay with BER molecular beacon; *G,* quantification of the assay performed using lineage negative cells extracts from WT and *Foxo3*$^{-/-}$ bone marrow (plot of mean ± S.D. of the normalized fluorescence signals) ($n = 6$; two independent experiments). Data expressed as mean ± S.D. Student's *t* test. *, $p < 0.05$; **, $p < 0.001$; ***, $p < 0.0002$; ****, $p < 0.0001$; *ns*, not significant.

might be compromised in *Foxo3*$^{-/-}$ LSK cells. Despite the increase in oxidative stress-mediated accumulation of damaged DNA (Fig. 2) and consistent with mitochondrial defects observed in Foxo3-null HSPC (36), apoptosis was increased only mildly but significantly in *in vitro* hydrogen peroxide-treated *Foxo3*$^{-/-}$ LSK cells, suggesting that *Foxo3*$^{-/-}$ LSK cells might exhibit some resistance to oxidative stress-mediated apoptosis (Fig. 5*E*).

To address a possible DNA repair defect, we used a recently developed (39) BER molecular beacon assay to quantitatively evaluate APE1 endonuclease activity and OGG1-mediated glycosylase activity for removal of the 8-oxo-dG lesion in an 8-oxo-dG/A base pair (Fig. 5*F*, *schematic*). Using this fluorescent real time quantitative assay, we found no difference in the APE1 endonuclease activity of WT and *Foxo3*$^{-/-}$ primitive hematopoietic cells (data not shown). However, compared with WT controls, the glycosylase activity of OGG1 in *Foxo3*$^{-/-}$ primitive hematopoietic cells was significantly reduced (Fig. 5*G*, $n = 6$, $p = 0.003$).

Despite using three different commercial (goat, rabbit, and mouse) anti-mouse OGG1 antibodies probing wild type and OGG1-deficient mouse embryonic fibroblasts (MEFs), we were unable to confirm their specific binding to OGG1 protein (data

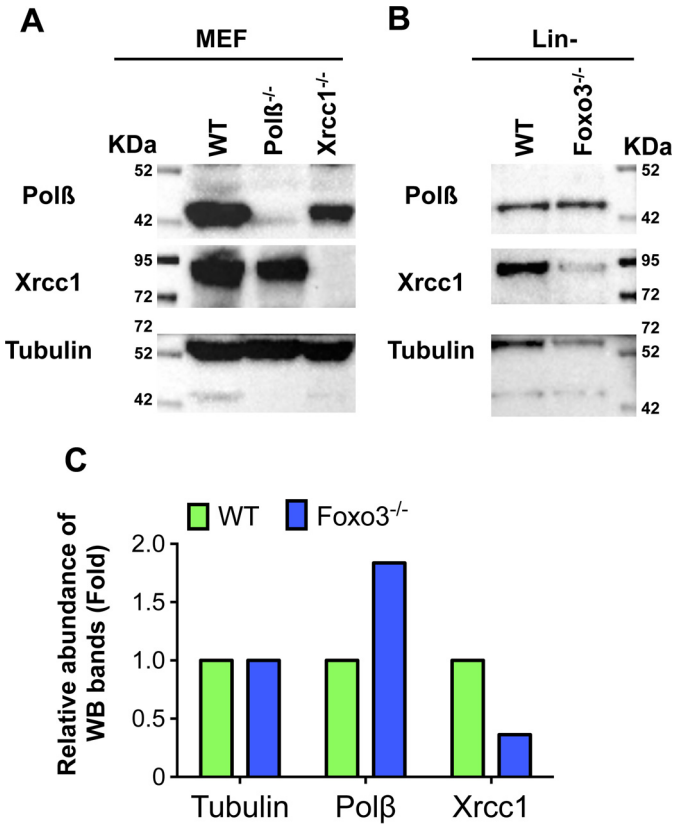

FIGURE 6. **Reduced expression of XRCC1 in the absence of Foxo3.** *A,* Western blotting analysis of pol β and XRCC1 in wild type (WT) and pol $\beta^{-/-}$ and XRCC1$^{-/-}$ MEFs, respectively. *B,* Western blotting analysis of pol β and XRCC1 in *Foxo3*$^{+/+}$ and *Foxo3*$^{-/-}$ lineage-negative bone marrow cells. *C,* protein quantification of pol β and XRCC1 relative to the level of expression in WT cells in *Foxo3*$^{-/-}$ lineage-negative bone marrow cells.

not shown). Using the same approach, we confirmed that anti-DNA *Polβ* and anti-XRCC1 antibodies specifically bind to their targets in wild type MEF but not in pol $\beta^{-/-}$ and XRCC1$^{-/-}$ MEFs, respectively (Fig. 6*A*). We further showed that whereas the expression of pol β is increased, the expression of XRCC1 is significantly reduced in HSPC in the absence of *Foxo3* (Fig. 6, *B*–*C*). XRCC1 is an essential element of base excision repair (40). Loss of FOXO3 may lead to discrepancies between mRNA and protein expressions (41, 42). Given the critical OGG1-XRCC1 interaction for BER, it is likely that reduced expression of XRRC1 mediates the defective OGG1 activity (43–45). Together with XRCC1 requirement for recruiting pol β to damaged DNA (46), these results support the notion that BER-mediated DNA repair in HSPC is dependent on FOXO3.

Foxo3$^{-/-}$ *Hematopoietic Stem and Progenitor Cells Respond Normally to Ionizing Radiation Insult*—To investigate *Foxo3*$^{-/-}$ HSPC response to additional insults, we used ionizing radiation (IR). LSK cells freshly isolated from WT and *Foxo3*$^{-/-}$ mice and kept *in vitro* displayed similar numbers of γH2AX nuclear foci 2 h after 10 Gy IR (Fig. 7*A*). In addition, WT and *Foxo3*$^{-/-}$ c-Kit^{+} hematopoietic progenitor cells responded similarly to 4 Gy IR, a dose to which HSPC are relatively tolerant (Fig. 7*B*) (47). More precise quantitative analysis by FACS 2 h after LSK and c-Kit^{+} multipotent progenitor cells were submitted to a 4 Gy IR dose confirmed that the capacity of *Foxo3*$^{-/-}$ HSPC in accumulating γH2AX is similar to WT cells (Fig. 7*B*). Similar results were obtained by *in vivo* total body irradiation (TBI). WT and *Foxo3*$^{-/-}$ LSK cells isolated 6 or 24 h after a 4 Gy TBI showed similar levels of DNA breaks (Fig. 7, *C* and *D*). Interestingly, although the expression of genes involved in homologous recombination (HR), such as *Brca1*, *Brca2*, and *Rad51,* was not modulated by the loss of FOXO3 in HSPC, genes implicated in the error-prone non-homologous end-joining pathway, which is the main repair mechanism of damaged DNA in HSPC (47) were significantly up-regulated in *Foxo3*$^{-/-}$ HSPC (Fig. 7*E*). Although the increased expression of XRCC6 (Ku70) (and possibly XRCC5 (Ku80)) might be part of a compensatory response (48), the source of this increase is unclear. These results suggest that loss of FOXO3 does not exacerbate ionizing radiation-induced DNA damage or alternatively does not compromise the DNA damage response machinery in response to ionizing radiation.

Altogether, our data identify FOXO3 as a regulator of DNA damage repair in HSPC under homeostasis and suggest that the observed DNA breaks (Figs. 1, *B*, *D*, and *E*, 2, 3, and 5*G*) are due to both an increase in endogenous ROS levels and a deficiency in oxidative DNA repair machinery in *Foxo3*$^{-/-}$ HSPCs (Fig. 8, *Model*).

Discussion

We showed here that *Foxo3*$^{-/-}$ HSPCs accumulate damaged DNA under homeostatic conditions. We also showed that the damaged DNA in homeostatic *Foxo3*$^{-/-}$ HSPCs is mediated by both elevated endogenous ROS and a defective base excision DNA repair program. Additionally, our data suggest that the *Foxo3*$^{-/-}$ HSC G_2/M delay is mediated primarily by elevated ROS. These results are consistent with and extend the scope of known FOXO3 (FOXO) functions in DNA damage response pathways (14, 48–50).

Our findings show that FOXO3 modulates a gene network related to BER and NER oxidative DNA repair, because a number of related genes are down-regulated in *Foxo3*$^{-/-}$ LSK cells (Fig. 5*A*). We were able to reveal oxidative DNA damage in *Foxo3*$^{-/-}$ hematopoietic stem and progenitor cells using the FLARE hOGG1 assay, in which the human OGG1 glycosylase is introduced into the comet assay to induce DNA breaks at locations of oxidative base lesions (Fig. 2). Furthermore, the hypersensitive BER molecular beacon assay that we recently developed (39) enabled us to show that OGG1-mediated glycosylase activity, which mediates the removal of the 8-oxo-dG lesion, is reduced in a population of *Foxo3*$^{-/-}$ hematopoietic cells enriched for stem and progenitor cells (Fig. 5, *F* and *G*). The reduction in OGG1 glycosylase activity in *Foxo3*$^{-/-}$ LSK was despite similar *Ogg1* transcript expression in *Foxo3*$^{-/-}$ as compared with WT LSK cells (Fig. 5*A*). Furthermore, we found that the expression of the XRCC1 protein, which is critical for BER, is highly reduced in *Foxo3*$^{-/-}$ Lin^{-} cells (Fig. 6, *B* and *C*). Interestingly, despite the reduction in transcript expression of both *XRCC1* and *Polβ*, only the XRCC1 protein was reduced in *Foxo3*$^{-/-}$ LSK cells (Fig. 6). As we had noted previously, the transcript expression in primary *Foxo3*$^{-/-}$ hematopoietic cells may not always fully correlate with the protein expression (41, 42). These results together implicate FOXO3 in the regulation of BER in hematopoietic stem and progenitor cells.

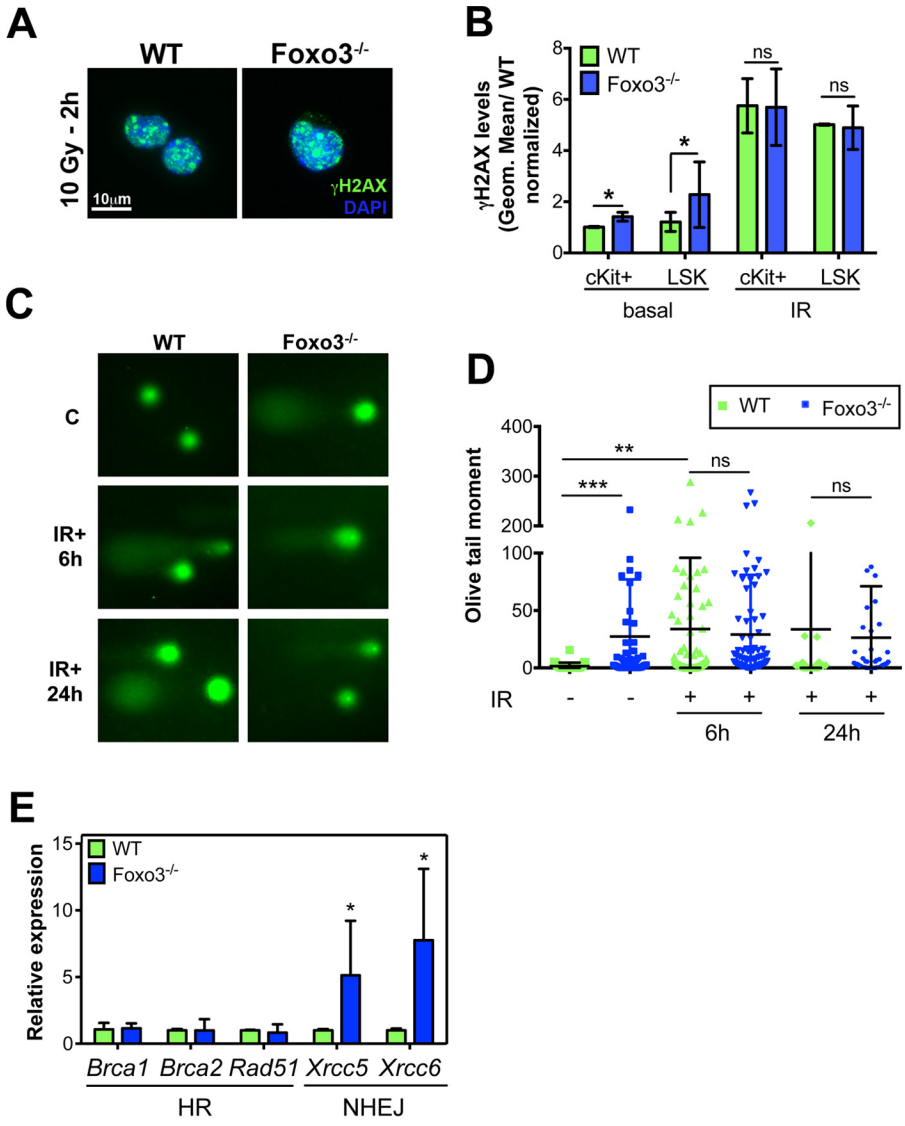

FIGURE 7. ***Foxo3*$^{-/-}$ hematopoietic stem and progenitor cells respond normally to ionizing radiation insult.** *A*, γH2AX staining on WT and *Foxo3*$^{-/-}$ LSK cells that were submitted to 10 Gy of ionizing radiation, kept in culture, and analyzed after 2 h. *B,* quantification of γH2AX levels by flow cytometry in WT and *Foxo3*$^{-/-}$ c-Kit^{+} and LSK cells 2 h after 4 Gy ionizing radiation dose ($n \geq 3$ per group). Plot presents geometric mean values of FITC fluorescence that were normalized to basal WT levels. *C,* representative comet assay pictures of LSK cells isolated from control (*C*) or 4 Gy irradiated (*IR*) WT and *Foxo3*$^{-/-}$ animals after 6 or 24 h and comet assay quantification (*D*). *E,* QRT-PCR analysis of DNA breaks repair genes involved in HR (*Brca1*, *Brca2,* and *Rad51*) or non-homologous end-joining (*Xrcc5* and *Xrcc6*) in *Foxo3*$^{-/-}$ c-Kit^{+} or LSK cells under homeostatic conditions. *Actnb* was used as an internal control, and expression was normalized to that of WT samples. Data are expressed as mean ± S.D. Student's *t* test. *, $p < 0.05$; **, $p < 0.001$; ***, $p < 0.0002$; *ns,* not significant.

These combined findings raise the possibility that compromised FOXO3 function, as it might occur in aging stem cells (33, 34) or in the context of stem cell malignancies, is likely to sustain damaged DNA and mitochondrial defects (36) and further contribute to stem cell aging and/or malignancy (18, 23, 29, 30, 32–34, 36). In agreement with this, FOXO3 inactivation is proposed to be one of the early events in the evolution of myeloid and perhaps other malignancies (18, 51). One of the implications of these combined results (36) is that elevated ROS, as a result of both mitochondrial defects and reduced anti-oxidant enzyme expression, contribute significantly to some, specifically to enhanced myeloproliferation, but not all of the main *Foxo3*$^{-/-}$ HSC defects. They also suggest that ROS-mediated *Foxo3*$^{-/-}$ HSC DNA damage may constitute a partially reversible phase in this process, because NAC treatment decreased DNA break levels and rescued HSPC from the cell cycle G_2/M delay (Figs. 3 and 4). However, potential clinical applications of these findings warrant careful consideration. As FOXO3 loss negatively affects the BER pathway (Fig. 5), the normalization of HSC cycling and G_2/M correction that followed antioxidant therapy (Fig. 4) might constitute only a transient response, in agreement with our recent report showing that NAC treatment is unable to rescue the long term reconstitution ability of *Foxo3*$^{-/-}$ HSC (36).

Data presented here, combined with published work (33, 34, 36, 52, 53), depict FOXO3 as a molecular node that wires together mitochondrial metabolism (36), ROS signaling, and DNA damage repair mechanisms for the maintenance of healthy HSPC. These collective findings join growing evidence in support of the notion that FOXO3 serves as a barrier to genomic instability in HSPC (52, 53).

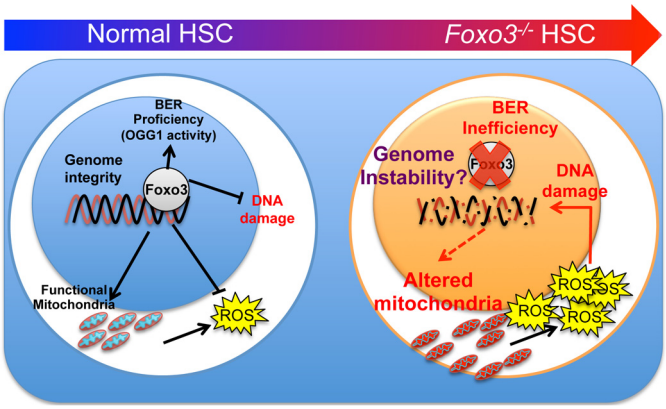

FIGURE 8. **Model of FOXO3 modulation of genomic integrity in hematopoietic stem and progenitor cells.** In normal HSPC, FOXO3 guards genome integrity by maintaining a gene expression program that represses ROS accumulation (anti-oxidant genes), promotes DNA repair (BER and NER genes), and sustains mitochondrial metabolism. *Foxo3*$^{-/-}$ HSPC accumulates defective mitochondria and elevates ROS and DNA damage leading to cell cycle impairment and potential genomic instability.

Experimental Procedures

Mice—All mice were from the C57BL/6 genetic background and were 10–12 weeks old (13). Protocols were approved by the Institutional Animal Care and Use Committee of the Icahn School of Medicine at Mount Sinai. NAC treatment was performed as described previously (13, 21).

Flow Cytometry and Hematopoietic Stem Cell Isolation—Antibody staining and bone marrow cell preparation for FACS sorting were performed as described previously (13, 21, 33). Briefly, for isolation of LSK and c-Kit^{+} cells, freshly isolated bone marrow cells were stained with biotinylated hematopoietic multiple lineage monoclonal antibody mixture (Stem Cell Technologies), PE-Sca-1, APC-c-Kit (BD Biosciences), and incubated with Pacific Blue^{TM} streptavidin secondary antibody. In addition to LSK staining and to isolate the long term HSC (LSK-Flk2^{-}CD34^{-}) , total bone marrow cells were stained with FITC-CD34 (eBioscience) and PE-Cy5-Flk2 (BD Biosciences) antibodies. Analyses and FACS sorting were performed at the Flow Cytometry Core at Icahn School of Medicine at Mount Sinai.

QRT-PCR—RNA from FACS-sorted c-Kit^{+} or LSK cells was extracted using the EasySep MicroPlus RNA extraction kit (Qiagen). RNA was retro-transcribed using SuperscriptII (Invitrogen) and cDNA corresponding to 300 cells was used per well for QRT-PCRs with specific primers (Table 1). QRT-PCRs were run on an ABI7900 thermal cycler (Applied Biosystems).

In Vitro Hydrogen Peroxide (H_2O_2) Treatment of LSK Cells—FACS-sorted WT and *Foxo3*$^{-/-}$ LSK cells were incubated in StemSpan SFEM (Stem Cell Technology) and treated with or without 100 μM of H_2O_2, washed extensively after 1 h, and either analyzed immediately (1 h) or cultured for further analyses at the indicated (2 and 4 h) time points by comet assay.

TBI—Mice were submitted to total body irradiation (4 Gy) (Icahn School of Medicine at Mount Sinai Irradiator Shared Resource Facility). Mice were sacrificed, and bone marrow cells were collected from non-irradiated controls or after 6 or 24 h post-TBI, and live LSK cells were FACS sorted and submitted immediately to comet assay.

Measurement of Intracellular ROS—ROS measurements were performed on freshly isolated bone marrow cells using 3 μM 2′,7′-dichlorofluorescein diacetate (Molecular Probes), as described previously (13, 21, 33).

Cell Cycle Analysis—Freshly isolated (2×10^6) bone marrow cells from *in vivo* BrdU-injected mice (one pulse, 19 h before sacrifice) were stained for LSK, fixed, permeabilized, and incubated with anti-BrdU antibody (Pharmingen) and co-stained with 7-AAD, following the manufacturer's instructions. Samples were immediately analyzed by flow cytometry. To measure the percentage of quiescent cells (G_0 phase), freshly isolated (2×10^6) bone marrow cells were stained for LT-HSC (LSK-CD34^{-}), fixed, permeabilized, incubated with anti-Ki67-PE-conjugated antibody (Pharmingen), and co-stained with 4′,6-diamidino-2-phenylindole (DAPI) (1 μg/ml).

Apoptosis Assay—Freshly FACS-sorted control and/or 1 h of H_2O_2-treated LSK cells were suspended in 1× annexin V-binding buffer containing 2.5 μl of annexin V-APC. Samples were co-stained with 7-AAD, following the manufacturer's instructions (BD Biosciences), and analyzed immediately by FACS.

γH2AX Analysis by Immunofluorescence Staining and Flow Cytometry—WT and *Foxo3*$^{-/-}$ FACS-sorted LSK cells were cytospun onto glass slides. γH2AX nuclear foci were analyzed by immunofluorescence staining using a rabbit polyclonal anti-phospho H2AX (Ser-139) (Millipore) and imaged on a Leica DMRA2 fluorescence microscope using ×400 oil immersion objective. Freshly isolated bone marrow cells stained for HSPC were fixed in 2% paraformaldehyde and stained overnight at 4 °C with 1:100 mouse monoclonal anti-H2AX pS139 FITC conjugate (Millipore) (or anti-H2AX pS139 APC conjugate, Biolegend) in BLOCK9 solution as described previously (54). The samples were next diluted into PBS, 2% FBS and analyzed by FACS.

Single Cell Gel Electrophoresis (Comet Assay) and FLARE^{TM} Assay—FACS-sorted LSK cells were submitted to alkaline comet assay using the Trevigen® CometAssay® kit following the manufacturer's instructions. Briefly, cells were mixed in melted agarose, placed in glass slides, and allowed to jellify at 4 °C for 30 min. After that, slides were subsequently immersed in lysis and unwinding solutions and immediately submitted to electrophoresis at 4 °C in an alkaline electrophoresis solution, pH 13. Finally, slides were dehydrated in 70% ethanol and allowed to dry before analysis.

For the FLARE hOGG1 assay, prior to the alkaline electrophoresis step, cells in agarose were incubated with a 1:2 dilution of human OGG1 glycosylase for 1 h at 37 °C to convert all oxidized bases into DNA breaks. Slides were analyzed on a Leica DMRA2 fluorescence microscope (×100 objective). Comet parameters were quantified using the CometScore software (TriTek Corp). The parameter percentage (%) of DNA in tail corresponds to the amount of pixels in the comet tail (migrated DNA), whereas the Olive tail moment (Olive *et al.*, (55)) corresponds to the product of the tail length and the fraction of DNA in the tail (intensity of the DNA in the tail).

DNA Oxidation Analysis—FACS-sorted LSK cells were incubated in the kit staining solution containing 1:20 dilution of a specific FITC-conjugated probe to 8-OHdG, in accordance

TABLE 1
Mouse primer sequences

Gene	Forward primer (5′ → 3′)	Reverse primer (5′ → 3′)
Apex1	TTATGGCATTGGCGAGGAAGA	CCAACGCTGTCGGTATTCCA
Brca1	TTGGAACTGATCAAAGAACCTGT	ACATTGTGAAGGCCCTTTCTT
Brca2	GGGAGTTGAAGTGGATCCTG	GGAGAGTCAGCAGGCGTTAC
Fen1	CACTGCTAGCTGCTTAAGGCT	GGAGCAATGGCTTCTTCCTACC
Lig1	GACGCCTGCTATCAATCGGT	ATCAGTTGTACCTTTTCCCTGGC
Lig3	CTTTTCAGCAGCAAAACCCAA	CGGAACTCTCGTAGCAGACA
Nthl1	CAAGATGGCACACTTGGCTA	CTCTTCTGGGGTCTTGGTCA
Ogg1	ATTCCAAGGTGTGAGACTGCT	ATGAGTCGAGGTCCAAAGGC
Parp1	CTTGAGCAGATGCCCTCCAA	CTCTTCGTCCTGGCCATAGTC
PolB	TCTGTCAAAGGGTGAAACAAAG	GATCTTTGGGGATCAACCTG
Pole3	CCCGAGGACCTAAATCTGCC	TTGCGAAGTTATTGGCACAGG
Rad51	AACCCATTGGAGGGAACATCA	GATTCTGGTCTCCCCTCTTCC
Xpa	AAAGCTACAGGTGGTAAAGCG	GCTTCTTATTGCTCGCCGC
Xpc	GTGGGCTGAGACCTTGAGAC	TGCACGCAATCCCTGGAATA
Xrcc1	TCTGTGGTCCTACAGTTGGAGA	AAAATGCGAACACGGTTGGG
Xrcc5	TTGGTGTAGCCTTCCCTTACA	GTATTGCCGCAAGTCTTCCA
Xrcc6	ACATGATGGAGTCGGAGCAA	ACTCATCTGCCAGGGAACC

with the manufacturer's instructions (OxyDNA assay kit, Calbiochem®).

Cell Pellet and Lysate Preparation for BER Molecular Beacon Assay—Approximately 6×10^6 lineage-negative (Lin−) cells from WT and *Foxo3*$^{-/-}$ mice (six mice per group) were collected and pelleted at 228 × *g* for 5 min. The cell pellets were washed once with PBS and then flash-frozen and kept at −80 °C. Whole cell lysates were prepared by a freeze-thaw method. Briefly, cells were resuspended in 150 μl of the BER molecular beacon reaction buffer (HEPES 25 mM, pH 7.8, KCl 150 mM, EDTA 0.5 mM, glycerol 1%, DTT 0.5 mM, 1× protease inhibitor (Pierce, catalog no. 539131)). The cell suspension was then frozen on dry ice for 5 min and then thawed in a 37 °C water bath for 5 min followed by vortexing at the maximum speed for 30 s. Cells were frozen and thawed for three cycles and then centrifuged at 16,400 rpm for 5 min to remove cellular debris. The protein concentration of each cell lysate was measured. Lysates were diluted with BER molecular beacon reaction buffer to a final concentration of 0.4 mg/ml and immediately used for the activity assay as detailed below (39).

BER Molecular Beacon Assay and Data Analysis—OGG1-mediated glycosylase activity was measured by a BER molecular beacon assay, essentially as we have described previously (39). Briefly, an OGG1 substrate (the 8-oxo-dG/A beacon, 5 μl, 200 nM) was added to the whole cell lysate (20 μl) that was prepared in BER molecular beacon reaction buffer (above). The reaction was performed at 37 °C using a StepOnePlus QRT-PCR machine (Applied Biosystems). Fluorescence was measured for three technical replicates every 20 s for 1 h and normalized to the signal from the completely denatured beacon within each well, as in previously published methods (39).

Western Blotting Analysis—Lineage-negative bone marrow depleted of mature cells and enriched for HSPC were lysed into 2× Laemmli buffer with 100 mM DTT. Proteins were resolved on SDS-PAGE, transferred to nitrocellulose membranes, and incubated with anti-POLB (1:3000) (Thermo Fisher, MA5-13899), anti-XRCC1 (1:3000; Bethyl, A300-065A), or anti-tubulin (1:1000; Calbiochem, CP06) replicates every 20 s for 1 h, normalized to the signal from the completely denatured beacon within each well, as in methods published previously (39).

Author Contributions—C. L. B. and S. G. conceived and designed the study, analyzed the data, and wrote the manuscript. C. L. B. performed the experiments with assistance from R. L. and P. R. J. L. performed and J. L. and R. W. S. designed and analyzed the experiments in Figs. 5*G* and 6 and contributed to the manuscript preparation.

Acknowledgment—We thank Valentina d'Escamard for technical help, the Flow Cytometry Core, and the Irradiator Shared Resource Facilities at the Icahn School of Medicine at Mount Sinai.

References

1. Lombard, D. B., Chua, K. F., Mostoslavsky, R., Franco, S., Gostissa, M., and Alt, F. W. (2005) DNA repair, genome stability, and aging. *Cell* **120,** 497–512
2. Rossi, D. J., Jamieson, C. H., and Weissman, I. L. (2008) Stems cells and the pathways to aging and cancer. *Cell* **132,** 681–696
3. Bigarella, C. L., Liang, R., and Ghaffari, S. (2014) Stem cells and the impact of ROS signaling. *Development* **141,** 4206–4218
4. Commoner, B., Townsend, J., and Pake, G. E. (1954) Free radicals in biological materials. *Nature* **174,** 689–691
5. Santos, M. A., Faryabi, R. B., Ergen, A. V., Day, A. M., Malhowski, A., Canela, A., Onozawa, M., Lee, J. E., Callen, E., Gutierrez-Martinez, P., Chen, H. T., Wong, N., Finkel, N., Deshpande, A., Sharrow, S., *et al.* (2014) DNA-damage-induced differentiation of leukaemic cells as an anti-cancer barrier. *Nature* **514,** 107–111
6. Walter, D., Lier, A., Geiselhart, A., Thalheimer, F. B., Huntscha, S., Sobotta, M. C., Moehrle, B., Brocks, D., Bayindir, I., Kastutnig, P., Muedder, K., Klein, C. E., Jauch, A., Schroeder, T., Geiger, H., *et al.* (2015) Exit from dormancy provokes DNA-damage-induced attrition in haematopoietic stem cells. *Nature* **520,** 549–552
7. Marty, C., Lacout, C., Droin, N., Le Couédic, J. P., Ribrag, V., Solary, E., Vainchenker, W., Villeval, J. L., and Plo, I. (2013) A role for reactive oxygen species in JAK2 V617F myeloproliferative neoplasm progression. *Leukemia* **27,** 2187–2195
8. Lagadinou, E. D., Sach, A., Callahan, K., Rossi, R. M., Neering, S. J., Minhajuddin, M., Ashton, J. M., Pei, S., Grose, V., O'Dwyer, K. M., Liesveld, J. L., Brookes, P. S., Becker, M. W., and Jordan, C. T. (2013) BCL-2 inhibition targets oxidative phosphorylation and selectively eradicates quiescent human leukemia stem cells. *Cell Stem Cell* **12,** 329–341
9. Svilar, D., Goellner, E. M., Almeida, K. H., and Sobol, R. W. (2011) Base excision repair and lesion-dependent subpathways for repair of oxidative DNA damage. *Antioxid Redox Signal* **14,** 2491–2507

10. Liang, R., and Ghaffari, S. (2014) Stem cells, redox signaling, and stem cell aging. *Antioxid. Redox Signal.* **20,** 1902–1916
11. Yahata, T., Takanashi, T., Muguruma, Y., Ibrahim, A. A., Matsuzawa, H., Uno, T., Sheng, Y., Onizuka, M., Ito, M., Kato, S., and Ando, K. (2011) Accumulation of oxidative DNA damage restricts the self-renewal capacity of human hematopoietic stem cells. *Blood* **118,** 2941–2950
12. Miyamoto, K., Araki, K. Y., Naka, K., Arai, F., Takubo, K., Yamazaki, S., Matsuoka, S., Miyamoto, T., Ito, K., Ohmura, M., Chen, C., Hosokawa, K., Nakauchi, H., Nakayama, K., Nakayama, K. I., et al. (2007) Foxo3a is essential for maintenance of the hematopoietic stem cell pool. *Cell Stem Cell* **1,** 101–112
13. Yalcin, S., Zhang, X., Luciano, J. P., Mungamuri, S. K., Marinkovic, D., Vercherat, C., Sarkar, A., Grisotto, M., Taneja, R., and Ghaffari, S. (2008) Foxo3 is essential for the regulation of ataxia telangiectasia mutated and oxidative stress-mediated homeostasis of hematopoietic stem cells. *J. Biol. Chem.* **283,** 25692–25705
14. Greer, E. L., and Brunet, A. (2008) FOXO transcription factors in ageing and cancer. *Acta Physiol.* **192,** 19–28
15. Eijkelenboom, A., Mokry, M., Smits, L. M., Nieuwenhuis, E. E., and Burgering, B. M. (2013) FOXO3 selectively amplifies enhancer activity to establish target gene regulation. *Cell Rep.* **5,** 1664–1678
16. Zhang, X., Yalcin, S., Lee, D. F., Yeh, T. Y., Lee, S. M., Su, J., Mungamuri, S. K., Rimmele, P., Kennedy, M., Sellers, R., Landthaler, M., Tuschl, T., Chi, N. W., Lemischka, I., Keller, G., and Ghaffari, S. (2011) FOXO1 is an essential regulator of pluripotency in human embryonic stem cells. *Nat. Cell Biol.* **13,** 1092–1099
17. Lee, J. Y., Nakada, D., Yilmaz, O. H., Tothova, Z., Joseph, N. M., Lim, M. S., Gilliland, D. G., and Morrison, S. J. (2010) mTOR activation induces tumor suppressors that inhibit leukemogenesis and deplete hematopoietic stem cells after Pten deletion. *Cell Stem Cell* **7,** 593–605
18. Ahn, J. S., Li, J., Chen, E., Kent, D. G., Park, H. J., and Green, A. R. (2016) JAK2V617F mediates resistance to DNA damage-induced apoptosis by modulating FOXO3A localization and Bcl-xL deamidation. *Oncogene* **35,** 2235–2246
19. Liang, R., Rimmelé, P., Bigarella, C. L., Yalcin, S., and Ghaffari, S. (2016) Evidence for AKT-independent regulation of FOXO1 and FOXO3 in haematopoietic stem and progenitor cells. *Cell Cycle* **15,** 861–867
20. Santo, E. E., and Paik, J. (2016) FOXO3a and haematopoietic stem cells: goodbye PI3K, hello SIRT1? *Cell Cycle* **15,** 879–880
21. Yalcin, S., Marinkovic, D., Mungamuri, S. K., Zhang, X., Tong, W., Sellers, R., and Ghaffari, S. (2010) ROS-mediated amplification of AKT/mTOR signalling pathway leads to myeloproliferative syndrome in Foxo3(−/−) mice. *EMBO J.* **29,** 4118–4131
22. Hillion, J., Le Coniat, M., Jonveaux, P., Berger, R., and Bernard, O. A. (1997) AF6q21, a novel partner of the MLL gene in t(6;11)(q21;q23), defines a forkhead transcriptional factor subfamily. *Blood* **90,** 3714–3719
23. Ghaffari, S., Jagani, Z., Kitidis, C., Lodish, H. F., and Khosravi-Far, R. (2003) Cytokines and BCR-ABL mediate suppression of TRAIL-induced apoptosis through inhibition of forkhead FOXO3a transcription factor. *Proc. Natl. Acad. Sci. U.S.A.* **100,** 6523–6528
24. Scheijen, B., Ngo, H. T., Kang, H., and Griffin, J. D. (2004) FLT3 receptors with internal tandem duplications promote cell viability and proliferation by signaling through Foxo proteins. *Oncogene* **23,** 3338–3349
25. Gu, T. L., Tothova, Z., Scheijen, B., Griffin, J. D., Gilliland, D. G., and Sternberg, D. W. (2004) NPM-ALK fusion kinase of anaplastic large-cell lymphoma regulates survival and proliferative signaling through modulation of FOXO3a. *Blood* **103,** 4622–4629
26. Chapuis, N., Park, S., Leotoing, L., Tamburini, J., Verdier, F., Bardet, V., Green, A. S., Willems, L., Agou, F., Ifrah, N., Dreyfus, F., Bismuth, G., Baud, V., Lacombe, C., Mayeux, P., and Bouscary, D. (2010) IκB kinase overcomes PI3K/Akt and ERK/MAPK to control FOXO3a activity in acute myeloid leukemia. *Blood* **116,** 4240–4250
27. Santamaría, C. M., Chillón, M. C., García-Sanz, R., Pérez, C., Caballero, M. D., Ramos, F., de Coca, A. G., Alonso, J. M., Giraldo, P., Bernal, T., Queizán, J. A., Rodriguez, J. N., Fernández-Abellán, P., Bárez, A., Peñarrubia, M. J., *et al.* (2009) High FOXO3a expression is associated with a poorer prognosis in AML with normal cytogenetics. *Leuk Res.* **33,** 1706–1709
28. Vandenberg, C. J., Motoyama, N., and Cory, S. (2016) FoxO3 suppresses Myc-driven lymphomagenesis. *Cell Death & Dis.* **6,** e2046
29. Sykes, S. M., Lane, S. W., Bullinger, L., Kalaitzidis, D., Yusuf, R., Saez, B., Ferraro, F., Mercier, F., Singh, H., Brumme, K. M., Acharya, S. S., Schöll, C., Tothova, Z., Attar, E. C., Frohling, S., *et al.* (2011) AKT/FOXO signaling enforces reversible differentiation blockade in myeloid leukemias. *Cell* **146,** 697–708
30. Naka, K., Hoshii, T., Muraguchi, T., Tadokoro, Y., Ooshio, T., Kondo, Y., Nakao, S., Motoyama, N., and Hirao, A. (2010) TGF-β-FOXO signalling maintains leukaemia-initiating cells in chronic myeloid leukaemia. *Nature* **463,** 676–680
31. Pellicano, F., Scott, M. T., Helgason, G. V., Hopcroft, L. E., Allan, E. K., Aspinall-O'Dea, M., Copland, M., Pierce, A., Huntly, B. J., Whetton, A. D., and Holyoake, T. L. (2014) The antiproliferative activity of kinase inhibitors in chronic myeloid leukemia cells is mediated by FOXO transcription factors. *Stem Cells* **32,** 2324–2337
32. Miyamoto, K., Miyamoto, T., Kato, R., Yoshimura, A., Motoyama, N., and Suda, T. (2008) FoxO3a regulates hematopoietic homeostasis through a negative feedback pathway in conditions of stress or aging. *Blood* **112,** 4485–4493
33. Rimmelé, P., Bigarella, C. L., Liang, R., Izac, B., Dieguez-Gonzalez, R., Barbet, G., Donovan, M., Brugnara, C., Blander, J. M., Sinclair, D. A., and Ghaffari, S. (2014) Aging-like phenotype and defective lineage specification in SIRT1-deleted hematopoietic stem and progenitor cells. *Stem Cell Reports* **3,** 44–59
34. Mehta, A., Zhao, J. L., Sinha, N., Marinov, G. K., Mann, M., Kowalczyk, M. S., Galimidi, R. P., Du, X., Erikci, E., Regev, A., Chowdhury, K., and Baltimore, D. (2015) The microRNA-132 and microRNA-212 cluster regulates hematopoietic stem cell maintenance and survival with age by buffering FOXO3 expression. *Immunity* **42,** 1021–1032
35. Zhang, X., Rielland, M., Yalcin, S., and Ghaffari, S. (2011) Regulation and function of FoxO transcription factors in normal and cancer stem cells: what have we learned? *Curr. Drug Targets* **12,** 1267–1283
36. Rimmelé, P., Liang, R., Bigarella, C. L., Kocabas, F., Xie, J., Serasinghe, M. N., Chipuk, J., Sadek, H., Zhang, C. C., and Ghaffari, S. (2015) Mitochondrial metabolism in hematopoietic stem cells requires functional FOXO3. *EMBO Rep.* **16,** 1164–1176
37. Kuo, L. J., and Yang, L. X. (2008) Gamma-H2AX- a novel biomarker for DNA double-strand breaks. *In Vivo* **22,** 305–309
38. Beerman, I., Seita, J., Inlay, M. A., Weissman, I. L., and Rossi, D. J. (2014) Quiescent hematopoietic stem cells accumulate DNA damage during aging that is repaired upon entry into cell cycle. *Cell Stem Cell* **15,** 37–50
39. Svilar, D., Vens, C., and Sobol, R. W. (2012) Quantitative, real-time analysis of base excision repair activity in cell lysates utilizing lesion-specific molecular beacons. *JoVE*, e4168
40. Caldecott, K. W. (2003) XRCC1 and DNA strand break repair. *DNA Repair* **2,** 955–969
41. Liang, R., Campreciós, G., Kou, Y., McGrath, K., Nowak, R., Catherman, S., Bigarella, C. L., Rimmelé, P., Zhang, X., Gnanapragasam, M. N., Bieker, J. J., Papatsenko, D., Ma'ayan, A., Bresnick, E., Fowler, *et al.* (2015) A systems approach identifies essential FOXO3 functions at key steps of terminal erythropoiesis. *PLoS Genet.* **11,** e1005526
42. Zhang, X., Campreciós, G., Rimmelé, P., Liang, R., Yalcin, S., Mungamuri, S. K., Barminko, J., D'Escamard, V., Baron, M. H., Brugnara, C., Papatsenko, D., Rivella, S., and Ghaffari, S. (2014) FOXO3-mTOR metabolic cooperation in the regulation of erythroid cell maturation and homeostasis. *Am. J. Hematol* **89,** 954–963
43. Ghosh, S., Canugovi, C., Yoon, J. S., Wilson D. M., 3rd, Croteau, D. L., Mattson, M. P., and Bohr, V. A. (2015) Partial loss of the DNA repair scaffolding protein, Xrcc1, results in increased brain damage and reduced recovery from ischemic stroke in mice. *Neurobiol. Aging* **36,** 2319–2330
44. Campalans, A., Moritz, E., Kortulewski, T., Biard, D., Epe, B., and Radicella, J. P. (2015) Interaction with OGG1 is required for efficient recruitment of XRCC1 to base excision repair and maintenance of genetic stability after exposure to oxidative stress. *Mol. Cell. Biol.* **35,** 1648–1658
45. Janik, J., Swoboda, M., Janowska, B., Ciesla, J. M., Gackowski, D., Kowalewski, J., Olinski, R., Tudek, B., and Speina, E. (2011) 8-Oxoguanine

incision activity is impaired in lung tissues of NSCLC patients with the polymorphism of OGG1 and XRCC1 genes. *Mutat Res.* **709–710**, 21–31
46. Fang, Q., Inanc, B., Schamus, S., Wang, X. H., Wei, L., Brown, A. R., Svilar, D., Sugrue, K. F., Goellner, E. M., Zeng, X., Yates, N. A., Lan, L., Vens, C., and Sobol, R. W. (2014) HSP90 regulates DNA repair via the interaction between XRCC1 and DNA polymerase β. *Nat. Commun.* **5,** 5513
47. Mohrin, M., Bourke, E., Alexander, D., Warr, M. R., Barry-Holson, K., Le Beau, M. M., Morrison, C. G., and Passegué, E. (2010) Hematopoietic stem cell quiescence promotes error-prone DNA repair and mutagenesis. *Cell Stem Cell* **7,** 174–185
48. Brenkman, A. B., van den Broek, N. J., de Keizer, P. L., van Gent, D. C., and Burgering, B. M. (2010) The DNA damage repair protein Ku70 interacts with FOXO4 to coordinate a conserved cellular stress response. *FASEB J.* **24,** 4271–4280
49. Huang, H., Regan, K. M., Lou, Z., Chen, J., and Tindall, D. J. (2006) CDK2-dependent phosphorylation of FOXO1 as an apoptotic response to DNA damage. *Science* **314,** 294–297
50. Tran, H., Brunet, A., Grenier, J. M., Datta, S. R., Fornace, A. J., Jr, Di Stefano, P. S., Chiang, L. W., and Greenberg, M. E. (2002) DNA repair pathway stimulated by the forkhead transcription factor FOXO3a through the Gadd45 protein. *Science* **296,** 530–534
51. Bigarella, C., Rimmele, P., Dieguez Gonzalez, R., Liang, R., Izac, B., Donovan, M., Papatsenko, D., and Ghaffari, S. (2013) Loss of p53 rescues the defective function of Foxo3−/− hematopoietic stem Cells but enhances their predisposition to malignancy. *Blood* **122,** 4199
52. Li, J., Du, W., Maynard, S., Andreassen, P. R., and Pang, Q. (2010) Oxidative stress-specific interaction between FANCD2 and FOXO3a. *Blood* **115,** 1545–1548
53. Li, X., Li, J., Wilson, A., Sipple, J., Schick, J., and Pang, Q. (2015) Fancd2 is required for nuclear retention of foxo3a in hematopoietic stem cell maintenance. *J. Biol. Chem.* **290,** 2715–2727
54. Muslimovic, A., Ismail, I. H., Gao, Y., and Hammarsten, O. (2008) An optimized method for measurement of gamma-H2AX in blood mononuclear and cultured cells. *Nat. Protoc* **3,** 1187–1193
55. Olive, P. L., Banáth, J. P., and Durand, R. E. (1990) Heterogeneity in radiation-induced DNA damage and repair in tumor and normal-cells measured using the comet assay. *Radiation Res.* **122,** 86–94